

Effect of the intermediate velocity emissions on the quasi-projectile properties for the Ar+Ni system at 95 A.MeV

D. Doré^{a,d¹}, Ph. Buchet^a, J.L. Charvet^a, R. Dayras^a,
 L. Nalpas^a, D. Cussol^b, T. Lefort^b, R. Legrain^a, C. Volant^a,
 G. Auger^c, Ch.O. Bacri^d, N. Bellaize^b, F. Bocage^b,
 R. Bougault^b, B. Bouriquet^c, R. Brou^b, A. Chbihi^c, J. Colin^b,
 A. Demeyer^e, D. Durand^b, J.D. Frankland^c, E. Galichet^{d,h},
 E. Genouin-Duhamel^b, E. Gerlic^e, D. Guinet^e, S. Hudan^c,
 P. Lautesse^e, F. Lavaud^d, J.L. Laville^c, J.F. Lecolley^b,
 C. Leduc^e, N. Le Neindre^b, O. Lopez^b, M. Louvel^b,
 A.M. Maskay^e, J. Normand^b, M. Parlog^f, P. Pawlowski^d,
 E. Plagnol^d, M.F. Rivet^d, E. Rosato^g, F. Saint-Laurent^{c²},
 J.C. Steckmeyer^b, M. Stern^e, G. Tabacaru^d, B. Tamain^b,
 L. Tassan-Got^d, O. Tirel^c, E. Vient^b, J.P. Wileczko^c

[INDRA Collaboration]

^a *DAPNIA/SPhN, CEA/Saclay, 91191 Gif-sur-Yvette Cedex, France*

^b *LPC Caen (IN2P3-CNRS/ISMRA et Université), 14050 Caen Cedex, France*

^c *GANIL (DSM-CEA/IN2P3-CNRS), B.P. 5027, 14076 Caen Cedex 5, France*

^d *IPN Orsay (IN2P3-CNRS), 91406 Orsay Cedex, France*

^e *IPN Lyon (IN2P3-CNRS/Université), 69622 Villeurbanne Cedex, France*

^f *Nuclear Institute for Physics and Nuclear Engineering, Bucharest, Romania*

^g *Dipartimento di Scienze Fisiche, Univ. di Napoli, 180126 Napoli, Italy*

^h *Conservatoire National des Arts et Métiers, 75141 Paris Cedex 03, France.*

¹ DAPNIA/SPhN, CEA/Saclay, 91191 Gif-sur-Yvette Cedex, France, e-mail: dore@in2p3.fr, FAX : 33.1.69.08.75.84

² present address : CEA, DRFC/STEP, CE Cadarache, 13108 Saint-Paul-lez-Durance, France

Abstract

The quasi-projectile (QP) properties are investigated in the Ar+Ni collisions at 95 A.MeV taking into account the intermediate velocity emission. Indeed, in this reaction, between 52 and 95 A.MeV bombarding energies, the number of particles emitted in the intermediate velocity region is related to the overlap volume between projectile and target. Mean transverse energies of these particles are found particularly high. In this context, the mass of the QP decreases linearly with the impact parameter from peripheral to central collisions whereas its excitation energy increases up to 8 A.MeV. These results are compared to previous analyses assuming a pure binary scenario.

Key words: PACS Numbers ; 24.10.-i, 25.70.-z

The Quasi-Projectile deexcitation has been studied through a wide variety of systems at intermediate energies [1]- [10]. In this energy domain a transition from a binary process, leading to two main excited fragments (the quasi-projectile (QP) and the quasi-target (QT)) in the exit channel, towards a participant-spectator mechanism, is expected. From inclusive or semi exclusive measurements it has not been possible to distinguish between these two mechanisms. In some cases, the experimental data could be described equally well either assuming a pure binary mechanism or a geometrical process [3],[11]. With the improvement of experimental setups, namely the advent of 4π multidetectors allowing fully exclusive measurements, it should become possible to reconstruct the QP and the QT from their decay products on an event by event basis. However, this reconstruction process depends greatly on our ability to identify unambiguously the origin of the detected products. Unfortunately, in the intermediate energy range, the various sources of emission strongly overlap in the velocity space. Thus one has to rely on some assumptions on the underlying mechanisms in order to unfold the various sources of emission. Although it was generally admitted that below 100 AMeV, heavy ion collisions have essentially a binary character, it has been shown since several years that the decay products could not be fully imputed to the decay of excited quasi-projectile and quasi-target [9]-[10],[12]- [18]. Besides preequilibrium and direct emissions already observed at low energies, processes like neck emission and aligned fission had to be taken into account in order to explain the experimental data. Indeed an excess of particles and fragments, not explained by the statistical deexcitation of fully equilibrated QP and QT, is observed at intermediate velocity with unusual kinematical properties.

From recent experimental data on the Ar+Ni reactions between 52 and 95 A.MeV obtained at GANIL with the 4π multidetector INDRA it was shown

[18] that it was not possible to reproduce the light particle rapidity spectra by assuming only statistical emissions from excited QP and QT and that there was an excess of high energy particles at mid-rapidity which increases as the impact parameter decreases. In the present paper, we will concentrate on the Ar+Ni reaction at 95 AMeV and we will show how the properties of the QP that one can extract from the data are strongly affected by particle emission around mid-rapidity. First the impact parameter classification and the event selection will be presented. Then, the QP properties, mass and excitation energy, will be established according to two basic assumptions. i) Neglecting mid-rapidity emission, following previous analysis [19]-[20], a two source reconstruction will be performed in the frame of a purely binary scenario. ii) In an attempt to take into account mid-rapidity emission (MRE) as evidenced in [18] we will unfold the experimental light charged particle rapidity spectra assuming three sources of emission, the QP, the QT and a third source of emission to simulate the mid-rapidity contribution. Thermal and shape equilibrium are assumed in each source. Then the properties of the QP are extracted from its decay products. In both cases, the mass and the excitation energy of the QP thus obtained will be presented as a function of an experimental impact parameter. Finally, results of both reconstruction methods will be compared and discussed.

The experiment was performed at the GANIL facility which provided an ^{36}Ar beam of $3-4 \times 10^7$ pps at 95 A.MeV. After collision with a $193 \mu\text{g}/\text{cm}^2$ self-supporting ^{58}Ni target, reaction products were detected with the 4π charged particle detector INDRA [21] with a minimum bias trigger requiring a four fold event. Charge identification is achieved up to the projectile charge in the forward hemisphere. Hydrogen and helium isotopes are separated for detection angles from 3^0 to 176^0 (rings 2 to 17).

Using the prescription of ref. [22], an impact parameter scale (b_{exp}) is deduced from the total transverse energy distribution (E_{tr}^{tot}) for all detected events as shown by the full line in Fig. 1(a). For the forthcoming analysis, we will retain only events for which, at least the remnant of the QP has been detected. This is done using the correlation between the total detected charge (Z_{tot}) and the pseudo total parallel momentum ($P_{//tot} = \sum Z_i \times V_{//i}$) presented in Fig. 1(b). Only events for which $P_{//tot} \geq 70\% P_{proj}$ are kept. This condition selects events with Z_{tot} around and larger than the projectile charge and represents $\approx 60\%$ of the estimated [23] total reaction cross section, σ_r^{th} , whereas the total detected one amounts to 80% of σ_r^{th} . We remark that the selected events (dashed line in Fig. 1(a)) still cover the whole range of E_{tr}^{tot} .

Proton and alpha particle reduced rapidity spectra (Y/Y_p where Y_p is the projectile rapidity) show two components centered respectively around the target

and the projectile velocities as shown in Fig. 2 for protons at $b_{exp}=6$ fm. This strongly suggests evaporation from excited QP and QT. Then, assuming a binary scenario and neglecting any non equilibrated emissions [19],[24], all particles and fragments are attributed to the QP or the QT event-by-event. The reconstruction is based on a simplified version of the thrust method [25]. Both procedures roughly allocate all particles and fragments with a parallel velocity smaller than the center-of-mass velocity to the QT and the others to the QP. Charges, masses and velocities of both sources are then calculated. Neutrons added in order to obtain the total mass of the system are distributed between the QP and the QT according to the N/Z ratio (=1.04) of the system. From simulations [26], the neutron kinetic energies are evaluated as the mean kinetic energy of the protons minus 2 MeV to take into account the absence of Coulomb barrier. Calorimetry is then used to calculate the excitation energy (E^*) of the QP. Event by event we have $E^* = \sum_i(m_i c^2 + E_i) - m_s c^2$, where m_i is the mass of each particle/fragment, E_i their kinetic energy in the QP frame and m_s the mass of the source. The mass of the QP thus reconstructed (around 34) is almost independent of the impact parameter. In contrast, the excitation energy per nucleon increases almost linearly with decreasing impact parameter to reach 18 A.MeV for central collisions. This value is in agreement with the one obtained in [20] for violent collisions. These results are shown by the full circles in Fig. 4 and will be further discussed in connection with the results of the second assumption.

It was shown in [18] that isotropic evaporation from excited QP and QT was not sufficient to explain the measured light products ($Z \leq 6$) rapidity spectra. In particular, there is an excess of particles emitted around mid-rapidity which cannot be explained by a simple overlap of the QP and QT emission spheres. This mid-rapidity contribution increases with decreasing b_{exp} . Furthermore, the average transverse energy ($\langle E_{tr} \rangle$) of these particles (fig. 3(a) full circles) is much higher than expected from evaporation. The same behaviour is observed for all products of $Z \leq 6$, suggesting that the excess of particles at intermediate velocity has peculiar kinematical properties. It has to be noted that due to detection thresholds, the $\langle E_{tr} \rangle$ values around the target rapidity are artificially increased.

In order to take into account this intermediate velocity component, besides the two evaporating sources, emission from a third source around mid-rapidity was assumed. A fit procedure, widely used to modelize differential cross sections [27–29], is performed supposing three thermalized sources. The laboratory energy spectra are fitted with the sum of three Maxwellian distributions assuming volume emission [30]:

$$d^2\sigma/dEd\Omega = \sum_{i=1,3} N_i \sqrt{E_l} \exp[-(E_l + Es_i - 2\sqrt{(E_l Es_i) \cos(\theta_l)})/T_i] \quad (1)$$

$N_i, E_{Si} = \frac{1}{2} M_{part} V_{source}^2$, T_i being adjustable parameters and E_l, θ_l and M_{part} are respectively the energy, the angle and the mass of the emitted particle in the laboratory. The number of parameters (9) can be reduced with the following assumptions : 1) the temperatures of the QP and of the QT are the same [31], 2) assuming that non equilibrium particles are emitted symmetrically around 90^0 in the center of mass, from momentum conservation, the QP and QT parallel velocities are linked through the relation $V_{QT} = (M_{proj}/M_{target})(V_{proj} - V_{QP})$.

Due to statistics, only energy spectra of light particles (p,d,t, ^3He , ^4He) are fitted. For each particle type, the detection energy thresholds are adjusted in order to have the same value for all rings (independently of the experimental thresholds which may fluctuate slightly from one detector to the other). For a given impact parameter bin and a given particle type, all energy spectra from ring 2 to ring 17 are fitted simultaneously [18]. As ring 1 ($2\text{-}3^0$) does not provide isotopic separation, it is not included in the fit. Thus, a set of parameters is obtained for each light particle type and each impact parameter bin. As shown in Fig. 3(b), the overall quality of the fits is quite good. Distribution irregularities are due to experimental biases. Solid angles are different from one ring to the other. The average angle of a ring being used to calculate the rapidity, the distributions are slightly distorted. For protons, at $b_{exp}=3$ fm, it is found that the mid-rapidity component contributes significantly to the total proton rapidity distribution and covers the whole rapidity range. Direct emissions evaluated with intranuclear cascade calculations give similar results [32]-[33]. One notes also that the average transverse energies, $\langle E_{tr} \rangle$ as a function of Y/Y_p are well reproduced (Fig. 3(a)).

The fit parameters for protons and alpha particles evolve rather smoothly with b_{exp} from central to peripheral collisions (see Table 1). The proton source reduced rapidities are rather constant from central to peripheral collisions for the QP ($0.91 < Y_{QP}/Y_p < 0.93$) and the mid-rapidity source ($0.46 < Y_{MRE}/Y_p < 0.49$). For other particles, both rapidities increase with impact parameter. The apparent temperature of the QP increases significantly from peripheral to central collisions (Table 1). At a given impact parameter, different particle types yield different temperatures in contradiction with the equilibrium hypothesis. In [31], similar deviations were observed and their possible origin discussed. It has been shown [34] that introducing nucleon-alpha scattering could improve significantly the fit for the alpha particle rapidity spectra. Thus, nucleon-cluster collisions in the region of overlap between projectile and target may be in part responsible for the discrepancies between the temperature parameters and source rapidities obtained in our simple three source fits for different particle types. For all particles, the apparent temperatures of the mid-rapidity source are large (Table 1) and increase strongly from peripheral to central collisions where they reach $\simeq 25\text{-}30$ MeV. These variations with impact parameter can be explained in part by the fact that the total transverse energy is used as

impact parameter selector. In effect, for instance, the temperature parameter is linked to the mean transverse energy through the relation $\langle E_{tr} \rangle = T$ for volume emission, thus establishing a correlation between the impact parameter selection and the temperature (see below).

The contribution of each source to the rapidity distribution depends upon the impact parameter and the particle type. The multiplicities of particles emitted by the QP and the QT follow the same evolution. The proton multiplicity for the QP (Table 1) stays constant around 1.5 from peripheral to mid-central collisions and then decreases to reach 0.5 in central collisions. For alpha particles, the multiplicity starts at a value of 0.5 in peripheral collisions to reach a maximum around 1.2 in mid-central collisions and then decreases to reach a value of 0.6 in central collisions. This behavior can be understood if the size of the source decreases with decreasing impact parameter while the temperature increases. For other particles the evolution is intermediate between that of protons and alpha particles. By contrast the multiplicity of particles emitted near mid-rapidity increases strongly as the impact parameter decreases whatever the particle type. This evolution suggests a geometrical effect as we will discuss later.

In order to evaluate the robustness of these results, several tests have been performed. Using different prescriptions to fit the data, constraining some of the parameters, adding Coulomb barriers, assuming surface emission instead of volume emission, lead essentially to the same evolution of the parameters (velocities, temperatures and multiplicities) with impact parameter. Assuming a surface emission for QP and QT, their source temperatures are found slightly lower but the fits are in poorer agreement with the experimental data. Using the heaviest fragment in the forward hemisphere, Z_{max} , as an indicator of the impact parameter (the closer to the charge of the projectile the fragment charge is, the larger is the impact parameter) avoids the correlation between the temperature and the impact parameter [34]. This procedure yields lower QP and QT temperatures but does not affect the relative contributions of each source. In [18], another global variable, related to the dissipated energy in the forward hemisphere, was used to select events according to the violence of the collision and emissions between 75° and 105° in the mid-rapidity frame were studied. In this case, the temperature parameters of the mid-rapidity evolved from 17 to 20 MeV for protons with the centrality of the collision. The event selection and the angular cut explain the differences between these results and those presented here. However, we remark that these values are located inside our limits (see Table 1).

The next step is the reconstruction of the QP as a function of impact parameter. The mean multiplicity and energy of each particle emitted by the QP at each impact parameter bin are used. Because the projectile has $N=Z$, neutrons are added assuming that neutron multiplicity is equal to proton multiplicity

($\langle mult_n \rangle = \langle mult_p \rangle$). The contribution of fragments at mid-rapidity being small, those are shared between the QP and the QT as in the two source analysis previously described. For a given impact parameter, the mass of the QP is calculated as,

$$\begin{aligned} \langle A_{QP} \rangle &= \Sigma_i \langle mult_i \rangle \times A_i + \Sigma_f \langle mult_f \rangle \times \langle A_f \rangle \\ &\quad + \langle mult_n \rangle \times A_n \end{aligned} \quad (2)$$

and its excitation energy is estimated through calorimetry,

$$\begin{aligned} \langle E_{QP}^* \rangle &= \Sigma_i \langle mult_i \rangle \times (m_i c^2 + \frac{3}{2} T_i) + \Sigma_f \langle mult_f \rangle \times (\langle m_f \rangle c^2 + \langle E_f \rangle) \\ &\quad + \langle mult_n \rangle \times (m_n c^2 + \frac{3}{2} T_p) - \langle m_{QP} c^2 \rangle \end{aligned} \quad (3)$$

where i, n, f are the index for light charge particles, neutrons and fragments and QP refers to the emitting source. A 's are the atomic masses, m 's, the masses, $\langle E_f \rangle$ are the fragment mean kinetic energies. Neutron temperature (T_n) is assumed to be equal to proton temperature (T_p). One can note that fragments have an important contribution in (2) due to their masses and a small one in (3) due to their low kinetic energies. All this reconstruction assumes that particles originate from the same source even if the velocities obtained with the fits are different. This difference being larger for small impact parameter, values below 3 fm are less significant.

The QP masses and excitation energies thus obtained, are presented (stars) in Fig. (4) as a function of the impact parameter, together with the results (circles) of the previous two source analysis. Whereas a two source analysis yielded QP masses independent of impact parameter, in contrast, for the three source approach, one notes in fig. 4 (a) a linear increase with impact parameter of the QP mass : from 10 for central collisions to 32 for peripheral ones. For peripheral collisions containing few mid-rapidity particles, both scenarii lead to nearly identical results. The linear mass increase with impact parameter suggests a geometrical dependence. In fig. 4(a) the curve represents the QP mass predicted in a calculation [2] where the geometrical overlap of projectile and target is considered as the intermediate source and the non interacting volumes are taken as QP and QT. Although the general trend with impact parameter is similar to the three source result, the predicted QP mass decreases more rapidly with decreasing b_{exp} than obtained from the three source analysis. This discrepancy at low impact parameter may be imputed, in part, to the b_{exp} determination. One can also argue that at 95 A.MeV the participant-spectator regime is not fully reached.

Dynamical calculations for small systems [9],[36]-[37] present a similar relation between the QP mass and the impact parameter if particles emitted before the

re-separation time of QP and QT are not included in the QP reconstruction. These calculations also show that these "early" particles are distributed over the whole range of parallel velocity as deduced from the three source fits. To obtain a realistic estimation of the QP emissions, it is important to subtract the mid-rapidity component over the whole rapidity range.

Excitation energies deduced from both analyses are compared in fig. 4 (b). The Z_{max} sorting (open symbols) has also been tested in order to roughly evaluate the effect of the event sorting. The Z_{max} value is the one corresponding to the more abundant QP residue in the considered b_{exp} bins. As observed, the obtained values are close to those of the three source fit method based on the b_{exp} sorting, indicating that the sorting has only small effect on the results. In all cases the excitation energies increase with decreasing impact parameter. However, except for the most peripheral collisions where mid-rapidity emission is negligible, the three source fit method yields excitation energies about a factor of two smaller than the two source analysis. As b_{exp} decreases, the mid-rapidity component carries an increasing amount of the deposited energy, limiting the excitation energy imparted to the QP and the QT.

Preliminary analyzes between 32 and 95 A.MeV [38] show that beyond 52 A.MeV the yields of the different sources become independent of the bombarding energy. The mean transverse energy of the mid-rapidity component increases linearly with bombarding energy while it is constant for the QP and QT contributions. Above ~ 50 A.MeV, most of the energy is deposited into the overlap region between projectile and target and is evacuated by the mid-rapidity particles.

Quasi-projectiles produced in the reaction $^{36}Ar + ^{58}Ni$ at 95 A.MeV have been reconstructed from their decay products under two basic assumptions, *i*) purely binary collisions, *ii*) additional emission from the overlapping zone between projectile and target. The properties (mass and excitation energy) of the QP thus reconstructed depend strongly upon these assumptions. Indeed, for mid-central collisions, there is a factor of 1.71 between QP masses and 1.76 between excitation energies, the assumption *ii*) leading to the lowest estimation. It has been shown that the properties of particles emitted at mid-rapidity are incompatible with an evaporation process from fully equilibrated quasi-projectiles and quasi-targets which made the assumption *i*) unrealistic. Based upon results of *ii*), these particles cover the whole rapidity range and mix in part with particles evaporated from the excited quasi-projectile and quasi-target. The unfolding procedure presented in this work is an important step in order to reconstruct sources with precision. The additional source in assumption *ii*) includes many processes and it will be necessary to disentangle them to go further in the interpretation.

References

- [1] D. Guerreau et al., *Nucl. Phys.* **A 447** (1985) 37c.
- [2] R. Dayras et al., *Nucl. Phys.* **A 460** (1986) 299.
- [3] R. Dayras et al., *Phys. Rev. Lett.* **62** (1989) 1017.
- [4] A. Badala et al., *Phys. Rev.* **C 48** (1993) 633.
- [5] J.E. Sauvestre et al., *Phys. Lett.* **B 335** (1994) 300.
- [6] A. Lleres et al., *Phys. Rev.* **C 50** (1994) 1973.
- [7] R. Laforest et al., *Nucl. Phys.* **A 568** (1994) 350 ; J. Pouliot et al., *Phys. Lett.* **B 299** (1993) 210 ; L. Beaulieu et al., *Phys. Rev. Lett.* **77** (1996) 462 ; M. Samri et al., *Phys. Lett.* **B 373** (1996) 40.
- [8] R.J. Charity et al., *Phys. Rev.* **C 52** (1995) 3126.
- [9] J. Péter et al., *Nucl. Phys.* **A 593** (1995) 95.
- [10] J.C. Angélique et al., *Nucl. Phys.* **A 614** (1997) 261.
- [11] D.J. Morrissey et al., *Phys. Rev. Lett.* **43** (1979) 1139.
- [12] C.P. Montoya et al., *Phys. Rev. Lett.* **73** (1994) 3070.
- [13] J.F. Dempsey et al., *Phys. Rev.* **C 54** (1996) 1710.
- [14] O. Dorvaux et al., *Nucl. Phys.* **A 651** (1999) 225.
- [15] J. Lukasik et al., *Phys. Rev.* **C 55** (1997) 1906 ; E. Plagnol et al., *Phys. Rev.* **C 61** (2000) 014606.
- [16] Y. Larochelle et al., *Phys. Rev.* **C 59** (1999) R565.
- [17] F. Bocage et al., *Nucl. Phys.* **A** , in press.
- [18] T. Lefort et al., *Nucl. Phys.* **A 662** (2000) 397.
- [19] M.F. Rivet et al., *Phys. Lett.* **B 388** (1996) 219 ; B. Borderie et al., *Phys. Lett.* **B 388** (1996) 224.
- [20] Y.-G. Ma et al., *Phys. Lett.* **B 390** (1997) 41.
- [21] J. Pouthas et al., *Nucl. Inst. Meth. Phys. Res.* **A 357** (1995) 418.
- [22] C. Cavata et al., *Phys. Rev.* **C 42** (1990) 1760.
- [23] S. Kox et al., *Nucl. Phys.* **A 420** (1984) 162.
- [24] V. Métivier et al., *Nucl. Phys.* **A 672** (2000) 357.
- [25] J. Cugnon et al., *Nucl. Phys.* **A 397** (1983) 519.

- [26] R.J. Charity et al., *Phys. Rev.* **46** (1992) 1951.
- [27] L. Phair et al., *Nucl. Phys.* **A548** (1992) 489.
- [28] U. Milkau et al., *Z. Phys.* **A346** (1993) 227.
- [29] W.C. Hsi et al., *Phys. Rev. Lett.* **73** (1994) 3367.
- [30] A.S. Goldhaber, *Phys. Rev. C* **17** (1978) 2243.
- [31] G. Lanzano et al., *Phys. Rev. C* **58** (1998) 281.
- [32] P. Pawłowski et al, submitted to *Phys. Rev. C*.
- [33] D. Doré et al., in preparation.
- [34] Ph. Buchet, Ph.D. Thesis, Université de Caen, 1999, unpublished.
- [35] G.D. Westfall et al., *Phys. Rev. Lett.* **37** (1976) 1202.
- [36] Ph. Eudes et al., *Phys. Rev. C* **56** (1997) 2003.
- [37] F. Haddad et al., *Phys. Rev. C* **60** (1999) 031603.
- [38] A. Hurstel et al., XXXVIIrd International Winter Meeting on Nuclear Physics, Bormio, Italy, 25-29 January 2000. Proceedings edited by I. Iori, Ricerca Scientifica ed Educatione Permanente Supplemento, p. 587.

	QP							MRE						
	Rapidity Y/Y _p		Temp. (MeV)		Mult			Rapidity Y/Y _p		Temp. (MeV)		Mult		
b (fm)	0-1	7-8	0-1	7-8	0-1	4-5	7-8	0-1	7-8	0-1	7-8	0-1	4-5	7-8
proton	0.91	0.93	8.4	5.0	0.5	1.6	1.5	0.46	0.49	25.5	15.0	6.3	2.6	0.3
alpha	0.82	0.95	14.4	6.9	0.6	1.2	0.5	0.46	0.71	30.1	8.4	2.9	0.8	0.2

Table 1

Fit parameters for protons and alpha particles in the quasi-projectile (QP) and the mid-rapidity component (MRE).

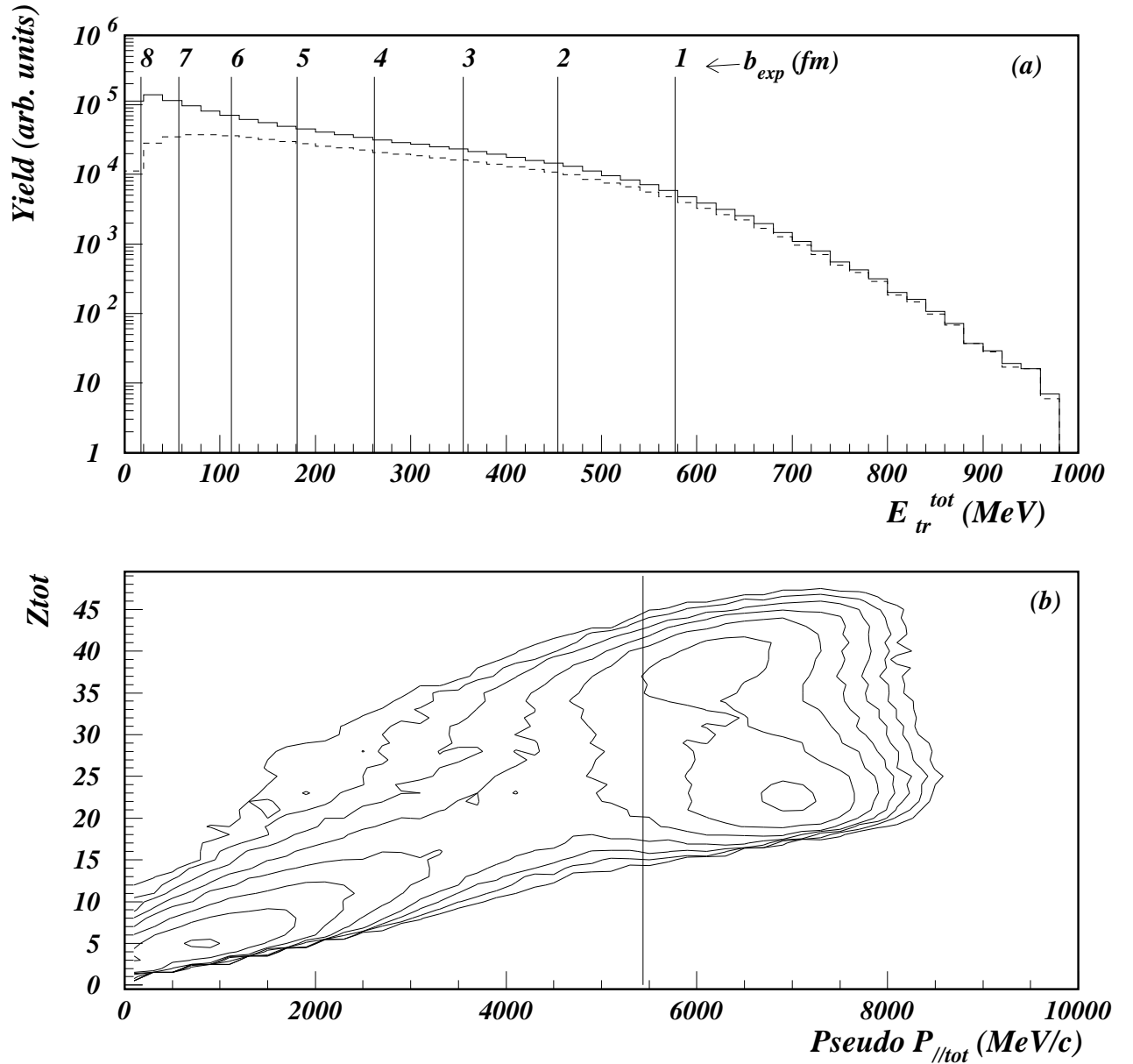


Fig. 1. (a) Total transverse energy distributions for all (full line) and selected events (dashed line). Estimated impact parameter values (in fm) corresponding to different E_{tr}^{tot} intervals are indicated. (b) Total charge versus pseudo total parallel momentum. Only events with a total momentum larger than 70 % of P_{proj} are selected (vertical line). There is a factor two between contour levels.

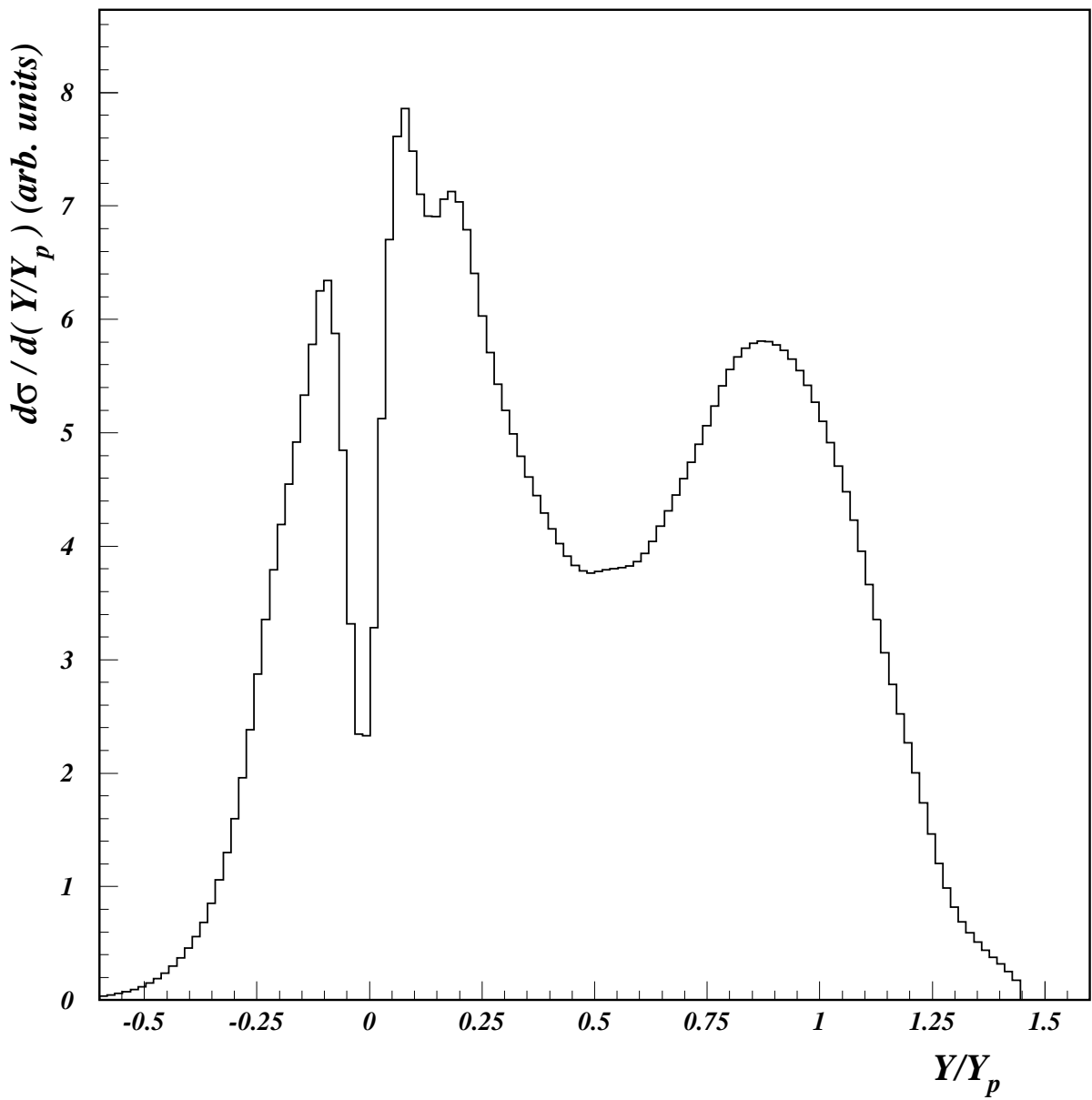


Fig. 2. Proton reduced rapidity distributions at $b=6$ fm. The hole at $Y/Y_p=0$ is due to the target shadow.

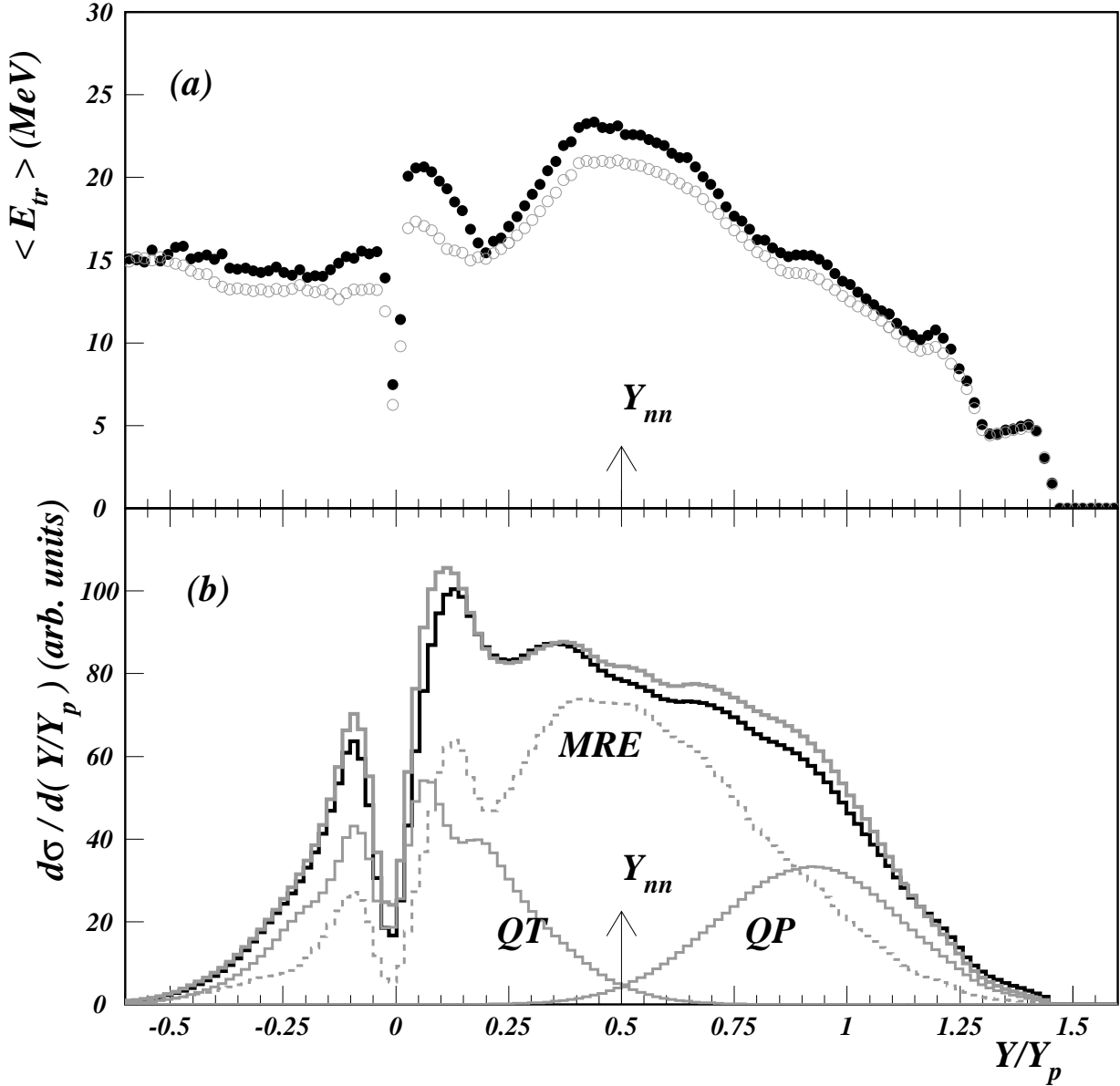


Fig. 3. Data and fit results for $b_{exp}=3$ fm. (a) Average transverse energy $\langle E_{tr} \rangle$ of protons vs reduced rapidity. The experimental data (full circles) are compared with the result of a three source fit (open circles). (b) Proton reduced rapidity distribution. The experimental data are indicated by the dark histogram and fit result by the grey line. The fit contributions of the QP, QT (grey lines) and the MR (dashed line) are drawn. The arrow labelled Y_{nn} indicates the nucleon-nucleon reduced rapidity. For experimental and calculated spectra, an energy threshold of 2 MeV was imposed.

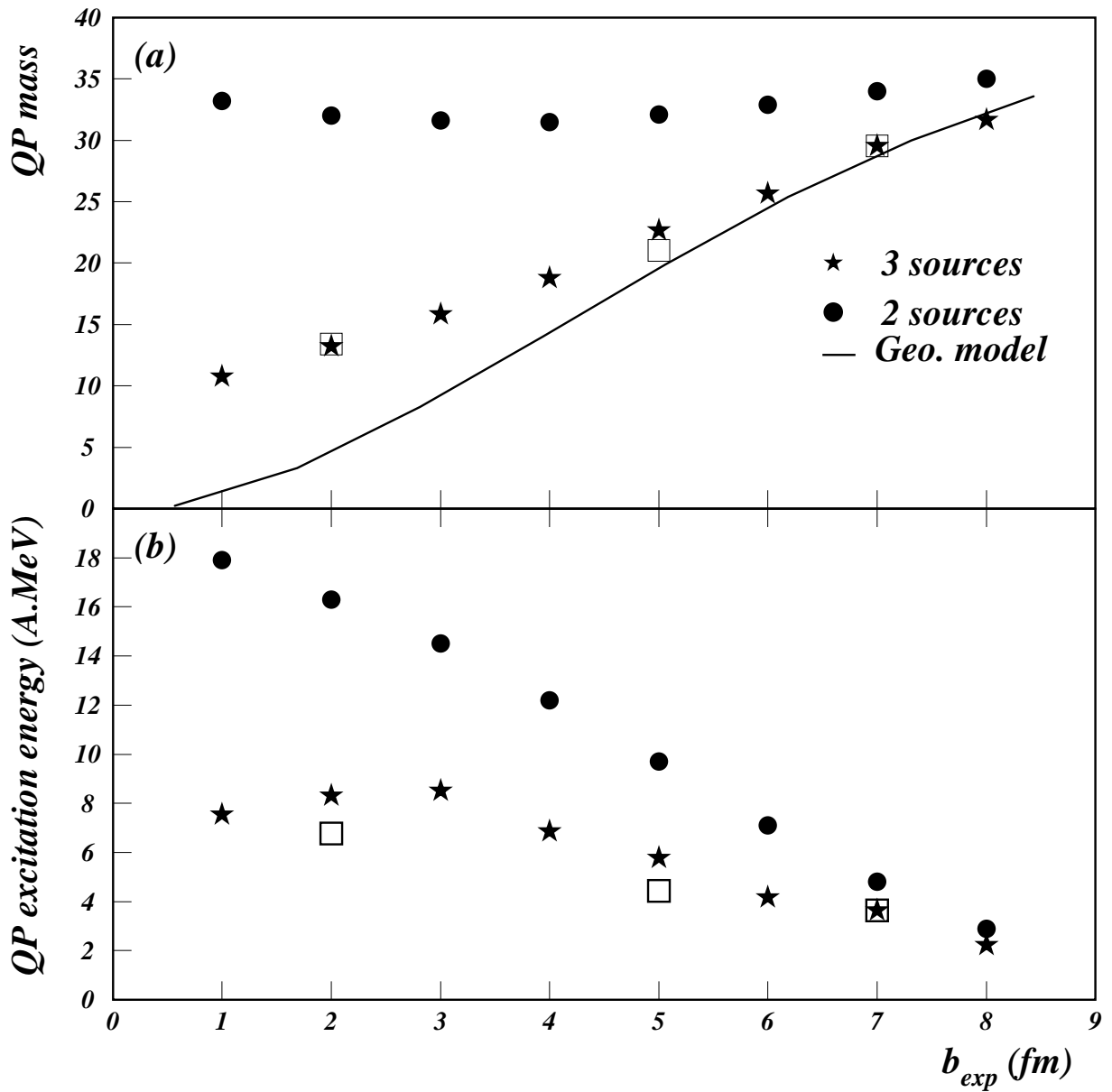


Fig. 4. Average QP mass (a) and excitation energy (b) as a function of the experimental impact parameter. The line in (a) is the result of a geometrical calculation (see text). Open symbols show the effect of the different event sortings.